



Quantitative Measurement of Hepatic Fibrosis with Gadoteric Acid-Enhanced Magnetic Resonance Imaging in Patients with Chronic Hepatitis B Infection: A Comparative Study on Aspartate Aminotransferase to Platelet Ratio Index and Fibrosis-4 Index

Guy Mok Lee, MD¹, Youe Ree Kim, MD¹, Jong Hyun Ryu, PhD², Tae-Hoon Kim, PhD², Eun Young Cho, MD, PhD³, Young Hwan Lee, MD¹, Kwon-Ha Yoon, MD, PhD^{1, 2}

Departments of ¹Radiology and ²Internal Medicine, Wonkwang University School of Medicine, Iksan 54538, Korea; ³Imaging Science Research Center, Wonkwang University, Iksan 54538, Korea

Objective: To quantitatively measure hepatic fibrosis on gadoteric acid-enhanced magnetic resonance (MR) in chronic hepatitis B (CHB) patients and identify the correlations with aspartate aminotransferase-to-platelet ratio index (APRI) and fibrosis-4 index (FIB-4) values.

Materials and Methods: This study on gadoteric acid-enhanced 3T MR imaging included 81 patients with CHB infection. To quantitatively measure hepatic fibrosis, MR images were analyzed with an aim to identify inhomogeneous signal intensities calculated from a coefficient of variation (CV) map in the liver parenchyma. We also carried out a comparative analysis between APRI and FIB-4 based on metaregression results. The diagnostic performance of the CV map was evaluated using a receiver-operating characteristic (ROC) curve.

Results: In the MR images, the mean CV values in control, groups I, II, and III based on APRI were 4.08 ± 0.92 , 4.24 ± 0.80 , 5.64 ± 1.11 , and 5.73 ± 1.28 , respectively ($p < 0.001$). In CHB patients grouped by FIB-4, the mean CV values of groups A, B, and C were 4.22 ± 0.95 , 5.40 ± 1.19 , and 5.71 ± 1.17 , respectively ($p < 0.001$). The mean CV values correlated well with APRI ($r = 0.392$, $p < 0.001$) and FIB-4 ($r = 0.294$, $p < 0.001$). In significant fibrosis group, ROC curve analysis yielded an area under the curve of 0.875 using APRI and 0.831 using FIB-4 in HB, respectively.

Conclusion: Gadoteric acid-enhanced MR imaging for calculating a CV map showed moderate correlation with APRI and FIB-4 values and could be employed to quantitatively measure hepatic fibrosis in patients with CHB.

Keywords: Liver; Magnetic resonance imaging; Chronic hepatitis B; Fibrosis; Gadoteric acid; Gd-EOB-DTPA

Received September 7, 2016; accepted after revision December 19, 2016.

This study was supported by a grant of the Korean Health Technology R&D Project, Ministry of Health & Welfare, Republic of Korea (HI12C0110).

Corresponding author: Kwon-Ha Yoon, MD, PhD, Department of Radiology, Wonkwang University School of Medicine, 460 Iksan-daero, Iksan 54538, Korea.

• Tel: (8263) 859-1005 • Fax: (8263) 859-1009
• E-mail: khy1646@wku.ac.kr

This is an Open Access article distributed under the terms of the Creative Commons Attribution Non-Commercial License (<http://creativecommons.org/licenses/by-nc/4.0>) which permits unrestricted non-commercial use, distribution, and reproduction in any medium, provided the original work is properly cited.

INTRODUCTION

Chronic hepatitis B (CHB) has a high prevalence in Asia. If left untreated, it can lead to serious conditions such as hepatocellular carcinoma (HCC), liver cirrhosis (LC), esophageal varices, or hepatic encephalopathy. In Korea, hepatitis B was the most common cause of the underlying liver diseases in HCC patients (1-4). The liver biopsy is a gold-standard modality for evaluating the hepatic fibrosis and its stage. However, repeated liver biopsy for fibrosis evaluation has several limitations, including sampling errors related to the sample size and complications such as pain and hemorrhage (5, 6). As such, there is a need

for a noninvasive evaluation of liver fibrosis. Noninvasive assessment methods of liver fibrosis can be divided into three categories: serological markers, fibrosis biomarkers, and imaging techniques. In many previous studies, multiple serological marker-based indices have been proposed, including aspartate aminotransferase (AST)-to-platelet ratio index (APRI), fibrosis-4 (FIB-4) score, age-platelet count index, and AST/alanine aminotransferase (ALT) ratio, and these have exhibited good correlations with the pathology of liver fibrosis (7-9). These indices are inexpensive and simple, as they incorporate routine laboratory results that are readily available in most of the hospital laboratories. Of the above-mentioned indices, APRI and FIB-4 provide an accurate assessment of liver fibrosis in CHB patients and are used as reference modalities for liver fibrosis (10). Recently, from a meta-analysis study, Xiao et al. (11) reported that APRI and FIB-4 possess moderate diagnostic accuracy for predicting fibrosis in patients with CHB viral infection. Among the serological markers, the two indices still could be considered as options for predicting fibrosis from CHB infection in regions with limited healthcare resources.

Gadolinium ethoxybenzyl diethylenetriaminepentaacetic acid or gadoxetic acid (Gd-EOB-DTPA) is an extracellular, hepatocyte-specific magnetic resonance imaging (MRI) contrast agent used to evaluate focal hepatic lesions such as HCC, cholangiocarcinoma, and hemangioma, as well as for liver perfusion, extracellular diffusion, and bile excretion analysis (11-14). This contrast agent is absorbed by organic anion transporting polypeptides (OATPB1/B3) and metabolized in hepatocytes during the hepatobiliary (HB) phase, which occurs approximately 15–20 minutes after injection (15-17). In LC, the expression level and activity of OATPB1/B3 are decreased, and the liver signal intensity in the HB phase is weaker in the cirrhotic portion relative

to the normal liver parenchyma, yielding decreased signal intensity and inhomogeneous enhancement during the HB phase. In previous studies, the histogram in HB phase was well correlated with liver fibrosis grade and this notion was supported by the fact that heterogeneity in HB phase may be correlated with liver fibrosis grade (16-19).

We hypothesized that we could suspect the degree of liver fibrosis by calculating liver enhancement heterogeneity in the HB phase, and accordingly, developed new MATLAB (R2012a, MathWorks, Natick, MA, USA)-based software to identify inhomogeneous signal intensities calculated from a coefficient of variation (CV) map to objectively quantify liver parenchymal heterogeneity.

In this paper, we aimed to evaluate the heterogeneity of liver parenchyma on Gd-EOB-DTPA-enhanced MR images, using CV value processed by our MATLAB-based software, and to demonstrate a correlation between the calculated heterogeneity and the calculated serologic markers including APRI and FIB-4, which have been known to have diagnostic accuracy for predicting hepatic fibrosis in CHB patients.

MATERIALS AND METHODS

Study Population

The local Institutional Review Board (IRB) approved this retrospective study and waived the requirement for written informed consent. A computer search identified a total of 138 patients with serologically confirmed CHB who underwent Gd-EOB-DTPA-enhanced MRI from December 1, 2013 to April 1, 2015 at our hospital. The exclusion criteria were inpatients that underwent Gd-EOB-DTPA-enhanced MRI (n = 32), patients who underwent a right lobectomy (n = 10), patient having scans with poor image quality (n = 6), and patients who did not undergo a laboratory study

Table 1. Demographic and Biochemical Characteristics of Patients Grouped by APRI Values

	Control (n = 36)	Group I (n = 17)	Group II (n = 46)	Group III (n = 18)
Age (years)				
All patients	56.8 (14–80)	56.8 (38–74)	57.8 (42–74)	59.2 (50–85)
Men	56.5 (14–75)	56.4 (38–74)	57.5 (42–74)	58.1 (50–85)
Women	57.3 (37–80)	57.5 (41–72)	59.1 (46–69)	63.0 (51–70)
Sex*				
Male	22 (61)	11 (65)	37 (80)	14 (78)
Female	14 (39)	6 (35)	9 (20)	4 (22)
AST level (IU/L)	28.4 (15–54)	23.7 (15–34)	40.6 (21–68)	66.9 (34–220)
Platelet count (10 ⁹ /L)	254 (102–529)	198.6 (133–331)	137.9 (73–231)	83.1 (42–357)

Unless otherwise indicated, data are presented in means, with range denoted in parentheses. *Data indicate numbers of patients, with percentages in parentheses. APRI = aspartate aminotransferase to platelet ratio index, AST = aspartate aminotransferase

Table 2. Demographic and Biochemical Characteristics of Patients Grouped by FIB-4 Values

	Control (n = 36)	Group A (n = 29)	Group B (n = 42)	Group C (n = 10)
Age (years)				
All patients	56.8 (14–80)	61.7 (47–85)	56.6 (42–74)	52.0 (38–63)
Men	56.5 (14–75)	60.7 (47–85)	56.6 (42–74)	49.3 (38–62)
Women	57.3 (37–80)	64.3 (51–70)	56.9 (46–72)	56.0 (41–63)
Sex*				
Male	22 (61)	22 (76)	34 (81)	6 (60)
Female	14 (39)	7 (24)	8 (19)	4 (40)
AST level (IU/L)	28.4 (17–33)	23.8 (15–34)	36.6 (21–65)	58.6 (30–220)
Platelet count (10 ⁹ /L)	254 (102–529)	207.1 (152–289)	151.0 (76–331)	96.6 (42–257)

Unless otherwise indicated, data are presented in means, with range denoted in parentheses. *Data indicate numbers of patients, with percentages in parentheses. AST = aspartate aminotransferase, FIB-4 = fibrosis-4

within 7 days from the MR study date (n = 9). Finally, 81 patients were included in the study (Tables 1, 2). Patients were divided into 3 subgroups according to their APRI: ≤ 0.5, non-significant fibrosis group (group I, n = 17); 0.5–1.4, significant fibrosis group (group II, n = 46); and ≥ 1.4, advanced fibrosis group (group III, n = 18) (9, 10). In addition, the patients were divided into control group and three groups based on FIB-4 threshold < 1.45 (group A, n = 29), 1.45–3.25 (group B, n = 42), and > 3.25 (group C, n = 10). Xiao et al. (11) cited this cut-off value in their study. None of the patients with CHB had a viral hepatitis C coinfection, biliary cirrhosis, Wilson disease, or autoimmune hepatitis. In addition, 36 patients without chronic liver disease who underwent Gd-EOB-DTPA-enhanced MRI during the study period were enrolled as the control group; colon cancer with liver metastasis (n = 11), biopsy for solitary hepatic tumor, which was confirmed benign tumor (n = 19).

All serologic data were obtained through laboratory studies conducted within 7 days from the Gd-EOB-DTPA-enhanced MRI study date. APRI and FIB-4 were calculated using the following formula:

$$\text{APRI} = \left(\frac{\left[\frac{\text{AST}}{\text{ULN}^*} \right]}{\text{platelet count [x } 10^9/\text{L}]} \right) \times 100$$

$$\text{FIB-4} = \frac{(\text{age [yr]} \times \text{AST [U/L]})}{(\text{platelet count [10}^9/\text{L]} \times \sqrt{\text{ALT [U/L]}})}$$

*The upper limit of normal (ULN) AST was 35 in this study.

MRI

Magnetic resonance imaging was performed on a 3T

scanner (Achieva; Philips Healthcare, Best, the Netherlands) with a 32-channel receiver body matrix coil. In all subjects, imaging was performed under fasting condition. All MR images were obtained in the axial plane, and T2-weighted images (WI) were additionally acquired in the coronal plane. The Gd-EOB-DTPA-enhanced MRI was performed before and after the administration of Gd-EOB-DTPA (Primovist; Bayer Healthcare, Berlin, Germany) and comprised of T1WI, acquired with a 3-dimensional T1 high-resolution isotropic volume excitation pulse sequence. Gd-EOB-DTPA (0.1 mL/kg body weight) was injected intravenously as a rapid bolus at a rate of 1.5 mL/s via a power injector (Sonic Shot 50; Nemoto Kyorindo Co., Ltd., Tokyo, Japan) while the patient was in the bore of the magnet. This was followed by a 15-mL flush with normal saline (1.5 mL/s). Arterial-phase imaging started after a modified scan delay with visual confirmation of contrast agent arrival in the abdominal aorta using a fluoroscopic triggering injection method. Subsequent contrast-enhanced-MRI was initiated at 50 seconds, 3 minutes, and 20 minutes (or HB phase) after the start of the bolus injection (13, 20).

Imaging Analysis and Measurement of Hepatic Fibrosis

To measure hepatic fibrosis quantitatively, we developed a MATLAB (R2012a, MathWorks, Natick, MA, USA)-based software to calculate a CV map, as suggested by Li et al. (21). The following procedure was used to calculate the CV map: bias correction of intensity inhomogeneity, followed by calculation of the CV map by dividing the CV value by each pixel value in the circular region of interest (ROI; diameter = 40 pixels) and, finally, calculating the mean value on the CV map (Fig. 1).

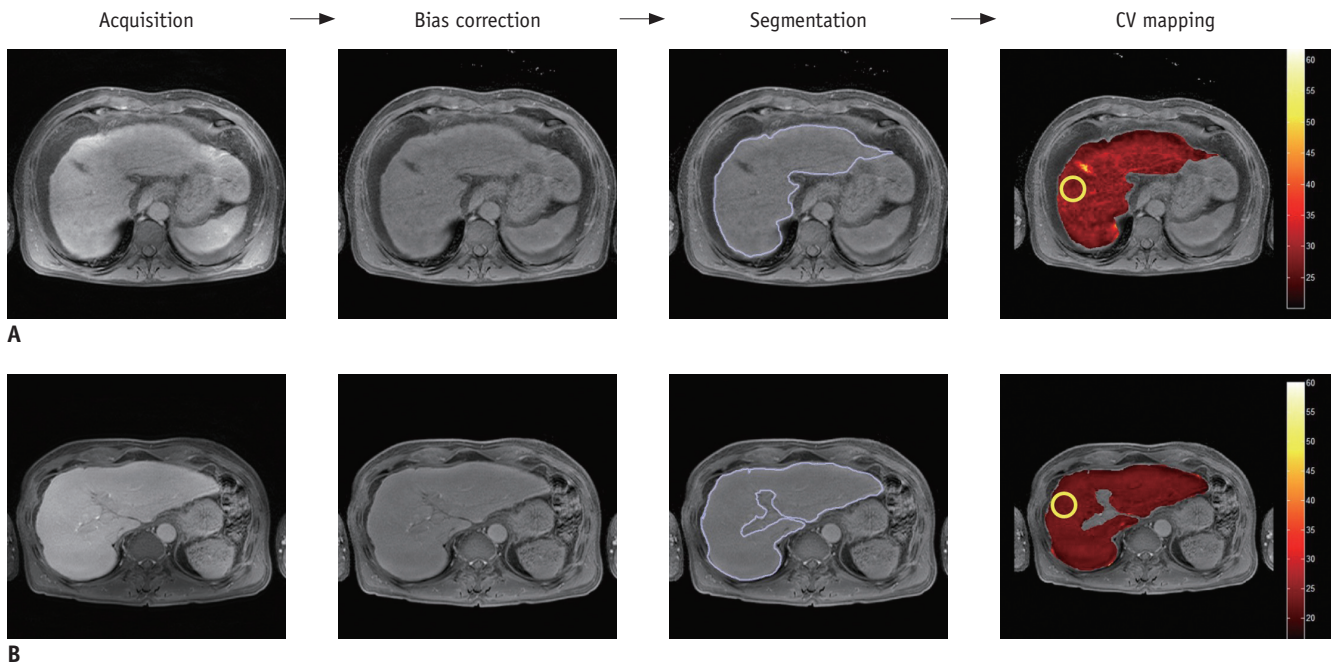


Fig. 1. Workflow for calculation of coefficients of variation (CV) in control subject (A) and in patient with chronic hepatitis B (B) in hepatobiliary phase of Gd-EOB-DTPA-enhanced MRI. To measure hepatic fibrosis quantitatively, MATLAB-based software was used to calculate CV map. After acquisition of MR images, bias correction and segmentation of liver parenchyma were performed, and then mean value of CV map on region of interest at anterior segment of right lobe of liver was calculated. Gd-EOB-DTPA = gadolinium ethoxybenzyl diethylenetriaminepentaacetic acid or gadoxetic acid, MRI = magnetic resonance imaging

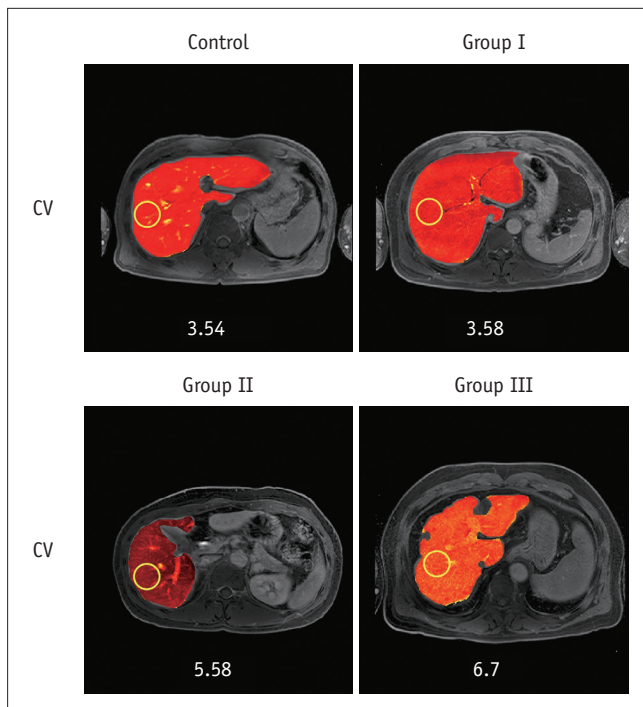


Fig. 2. Images show representative CV maps on control and patients with chronic hepatitis B of group I, II, and III on HB phases of Gd-EOB-DTPA-enhanced MRI. CV values are 3.54, 3.58, 5.58, and 6.7 in HB phase, respectively. CV = coefficients of variation, Gd-EOB-DTPA = gadolinium ethoxybenzyl diethylenetriaminepentaacetic acid or gadoxetic acid, HB = hepatobiliary, MRI = magnetic resonance imaging

$$CV = \frac{\text{Standard deviation}}{\text{Mean}} \times 100$$

$$CV \text{ Map} = \frac{CV}{\text{Pixel value}} \times 100$$

Gd-EOB-DTPA-enhanced axial images obtained during the HB phase MR image were obtained in Digital Imaging and Communications in Medicine format and stored on console containing the MATLAB-based program. For quantitative measurements of liver parenchymal heterogeneity, two abdominal radiologists (with 24 years of experience and with 4 years of experience in abdominal imaging), blinded to clinical information and pathological fibrosis grades, performed the procedure by positioning separate circular ROIs (diameter = 40 pixels) on the selected MR images, which was bias-corrected. In all subjects, ROIs were placed on the anterior segment of the right hepatic lobe with no overlap over large vessels and focal lesions such as cysts or tumors (Fig. 2). Each radiologist measured ROIs 3 times in the selected MR images and calculated the mean.

Statistical Analysis

The relationships between the CV values on HB-phase images and APRI and FIB-4 were evaluated using nonparametric Spearman correlation coefficients.

Comparisons of CV values between the control group and CHB groups I, II, or III and between the control group and CHB groups A, B, or C were performed using the Kruskal-Wallis test and intergroup comparisons were performed using the Mann-Whitney test. The diagnostic performance of CV with respect to significant liver fibrosis was evaluated using a receiver-operating characteristic (ROC) curve and calculated two times; the first one was for the APRI version (> 0.5) and the second one was for the FIB-4 version (> 1.45). The ROC curve is a plot of the sensitivity versus (100-specificity) values at all possible cut-off values. Optimal cut-off values were selected using a common optimization step that maximized the Youden index for predicting significant fibrosis; sensitivity and specificity were calculated from the same data without further adjustments. The inter-observer agreement was performed based on the intraclass correlation coefficient. The Kruskal-Wallis test, Mann-Whitney test, Spearman correlation

Table 3. Mean Values of Coefficients of Variation (CV) in Liver Parenchyma in Hepatobiliary Phase Images among Control and Chronic Hepatitis B Groups by Using APRI and FIB-4

APRI	CV Value	FIB-4	CV Value
Control group	4.08 ± 0.92	Control group	4.08 ± 0.92
Group I	4.24 ± 0.80	Group A	4.22 ± 0.95
Group II	5.64 ± 1.11	Group B	5.40 ± 1.19
Group III	5.73 ± 1.28	Group C	5.71 ± 1.17

Data are shown as means \pm standard deviations. APRI = aspartate aminotransferase-to-platelet ratio index, FIB-4 = fibrosis-4

coefficients, and intraclass correlation coefficient were conducted using SPSS version 18.0 (SPSS Inc., Chicago, IL, USA) and ROC, sensitivity, and specificity were analyzed with MedCalc version 15.6 (MedCalc, Mariakerke, Belgium).

RESULTS

The mean CV and APRI values for the control and CHB groups are listed in Table 3. In the HB phase of enhanced T1WI, the mean CV values of control and patients in groups I, II, and III by APRI were 4.08 ± 0.92 , 4.24 ± 0.80 , 5.64 ± 1.11 , and 5.73 ± 1.28 , respectively ($p < 0.001$) and the mean CV values of control and patients in groups A, B, and C by FIB-4 were 4.08 ± 0.92 , 4.22 ± 0.95 , 5.40 ± 1.19 , and 5.71 ± 1.17 , respectively ($p < 0.001$). The CV values in groups II and III were significantly higher than the values in the control group and group I ($p < 0.001$). The comparative analysis of CV values among the control group and CHB groups revealed higher mean CV values in CHB group III/C, followed by those in CHB group II/B, CHB group I/A, and the control group, and these differences were significant ($p < 0.001$) (Table 3). Pairwise comparisons of CHB groups I/A and II/B with respect to HB phase MR images revealed very significant results ($p < 0.001$).

An analysis of the relationship between the CV with the APRI and FIB-4 among patients with CHB revealed moderate correlations; r value for APRI and FIB-4 was 0.392 and 0.294, respectively (Fig. 3). ROC curves for the CVs in CHB patients

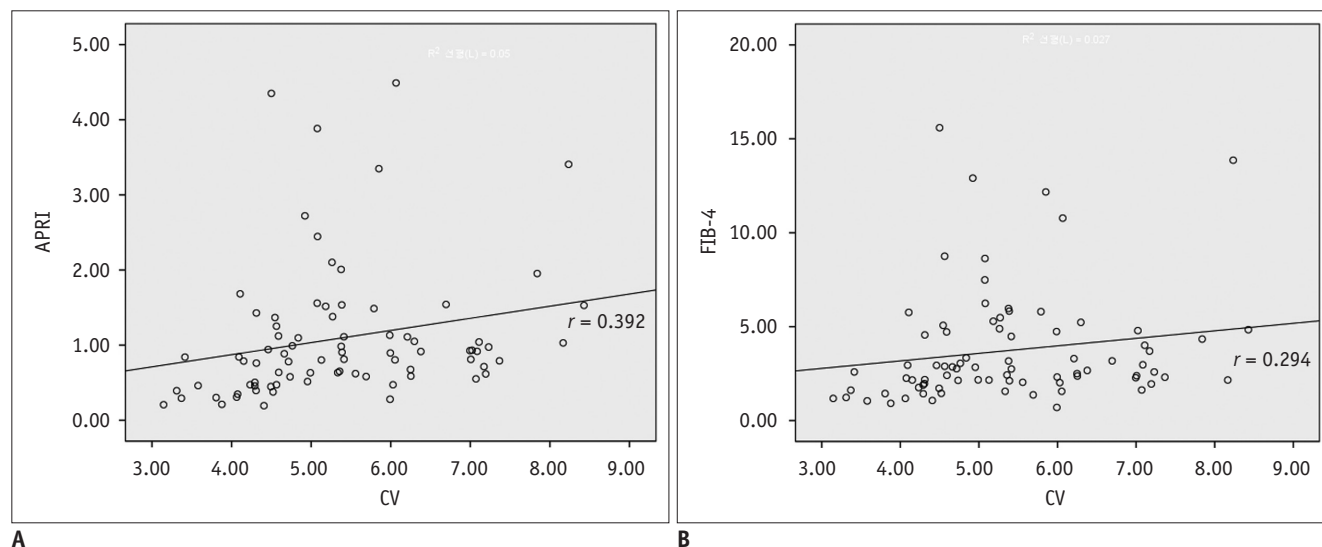


Fig. 3. Correlation of CV with APRI and FIB-4.

A. Shows correlation between aspartate aminotransferase-to-platelet ratio and coefficient of variation (CV) ($r = 0.392$, $p < 0.001$). **B.** Shows correlation between FIB-4 and CV values ($r = 0.294$, $p < 0.001$) in HB phases of Gd-EOB-DTPA-enhanced MRI. FIB-4 = fibrosis-4, Gd-EOB-DTPA = gadolinium ethoxybenzyl diethylenetriaminepentaacetic acid or gadoxetic acid, HB = hepatobiliary, MRI = magnetic resonance imaging

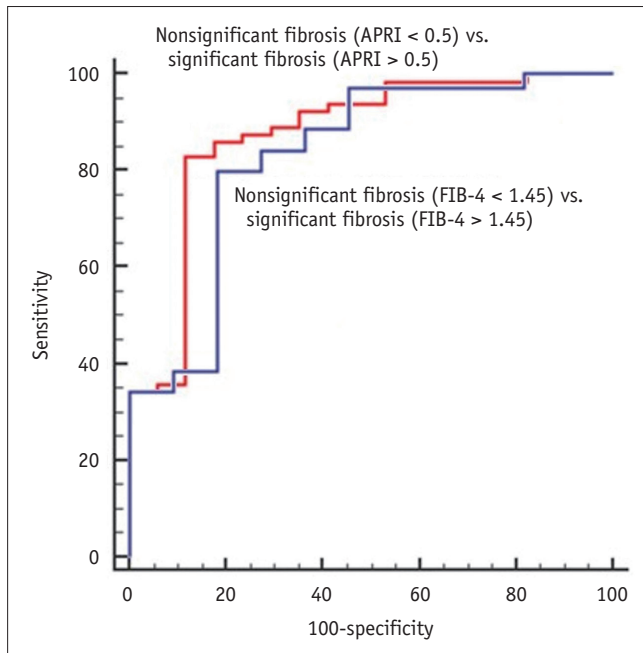


Fig. 4. Receiver operating characteristic curves of coefficient of variation used for diagnosis in patient with significant fibrosis (aspartate aminotransferase-to-platelet ratio > 0.5 and FIB-4 score > 1.45). AUC was 0.875 in APRI version with optimal cut-off values of 4.1866 (red line). AUC was 0.831 in FIB-4 version with optimal cut-off values of 4.5642 (blue line). APRI = aspartate aminotransferase to platelet ratio index, AUC = area under the curve, FIB-4 = fibrosis-4

Table 4. Cut-Off and Diagnostic Performance Values of Coefficient of Variation (CV) in Patients with Chronic Hepatitis B and Significant Fibrosis by Using APRI and FIB-4

	APRI	FIB-4
Cut-off value of CV	> 4.19	> 4.56
Sensitivity (%)	82.8	80.0
Specificity (%)	88.2	81.8
AUC	0.875	0.831
<i>p</i>	< 0.001	< 0.001

APRI = aspartate aminotransferase-to-platelet ratio index, AUC = area under the curve, FIB-4 = fibrosis-4

with or without significant fibrosis are described in Figure 4 and Table 4. The area under the curve (AUC) was 0.875 in APRI version with an optimal cut-off value of 4.19 for predicting significant fibrosis in the HB phase. The sensitivity and specificity at the optimal cut-off values of the HB phase were 82.8 and 88.2%, respectively. Secondly, the AUC was 0.831 in FIB-4 version with an optimal cut-off value of 4.56. The sensitivity and specificity at the optimal cut-off values were, 80.0 and 81.8%, respectively on the HB phase. The intraclass correlation coefficient between the two radiologists was 0.947 (95% CI, 0.918–0.966) in HB phase image.

DISCUSSION

Gd-EOB-DTPA is a liver-specific contrast agent. Gd-EOB-DTPA transport from the sinusoids to hepatocytes is mostly mediated by OATP1/B3, and its excretion into the bile duct is mediated by the multidrug resistance protein 2 (MRP2) (21-26). Progressive liver fibrosis has been reported to reduce OATP1/B3 activity and features the activation of collagen-producing hepatic stellate cells, collagen deposition in the subendothelial space of Disse, and all of which may promote the development of a fibrotic barrier in the liver parenchyma and reduced Gd-EOB-DTPA uptake (27-29). It was also supported by another literature. In a study by Tsuda and Matsui (29), higher levels of MRP2 activity were observed in cirrhotic rats, indicating that advanced liver fibrosis may lead to earlier Gd-EOB-DTPA excretion. Therefore, the absence of even distribution of Gd-EOB-DTPA in all liver parenchymal compartments and hepatocytes has been observed after administration of the contrast agent to CHB patients, thus leading to inhomogeneous enhancement of the liver parenchyma.

Our results revealed a significant difference in mean CV values between CHB groups I/A and II/B. This finding indicates that heterogeneous liver parenchymal enhancement is helpful in determining the presence of significant fibrosis in patients with CHB. We found the diagnostic accuracy of CV value, which is comparable to APRI and FIB-4 for predicting CHB-related fibrosis. The results showed that CV had ROC values of 0.875 in APRI version and 0.831 in FIB-4 version. The results suggested that the CV value had modest accuracy for detecting significant fibrosis. The AUC results from another previous study on quantification of liver fibrosis in CHB by imaging modality were similar to our results. For example, in a meta-analysis of the fibroscan in CHB, the AUC for the diagnosis of significant fibrosis (F2) was 0.859 (30). In a study by Shi et al. (31), MR elastography demonstrated good diagnostic performance for \geq F2 (AUC values was 0.986) and the value was higher than our results.

The CV measurements of liver fibrosis are associated with many advantages. First, this type of liver fibrosis assessment is very simple and does not require new imaging equipment. Recently, MR elastography, ultrasonographic elastography, and fibroscan were developed for liver fibrosis evaluation. However, all of these techniques require new imaging equipment, thus placing a restriction on access (32, 33). Second, CV mapping does not require any additional

MR scanning. This technique is mediated by software and objectively quantifies liver parenchymal heterogeneity. Third, heterogeneity measurements require only Gd-EOB-DTPA-enhanced MRI, which includes information about the liver function and simultaneously facilitates HCC screening. Fourth, measurement using CV mapping is highly reproducible, which is revealed by a high inter-observer agreement of 0.947 between the most experienced radiologist and one with less experience. Any radiologist or clinician can use the CV value on HB phase MR image by following simple instructions using this software.

Nowadays, Gd-EOB-DTPA enhanced MRI has become popular and has revealed high diagnostic accuracy for HCC surveillance. Based on our results, it is hypothesized that the CV values would impart an additional value for Gd-EOB-DTPA-enhanced MR in predicting advanced hepatic fibrosis or cirrhosis, and a radiologist or clinician could pay attention to the patients with high CV values. Further study is needed for analyzing the correlation between CV values and pathologic fibrosis grades.

When this study was designed, only outpatients were enrolled as laboratory data are influenced by the patient's general condition. Moreover, many patients with CHB and advanced LC had comorbid HCC, ascites, or portal hypertension and were treated with various drugs, including chemotherapeutic agents. These drugs are metabolized in the liver and cause liver toxicity. Accordingly, we wanted to exclude other potential influences on AST or platelet levels and therefore included only outpatients in our study.

This study has several limitations. First, LC and normal liver parenchyma were not histologically confirmed in our patient population, as the patients were followed up using noninvasive evaluations such as blood tests or imaging modalities, and only a few patients with CHB who had special indications underwent liver biopsy at our hospital. As a result, we depended on clinical data to obtain a reference degree of liver fibrosis and evaluated the heterogeneity of liver enhancement effects based on APRI and FIB-4, rather than on the histological grading of fibrosis. Second, we positioned the ROI at the right anterior or posterior segment of the liver (segments 5/6 and 7/8) because this area does not contain major vessels and is far from the heart, thus reducing the incidence of cardiac motion artifacts. However, the CV of the ROI area is not representative of the whole liver, and thus some selection bias might have occurred. Third, this was a retrospective study and the APRI and FIB-4 values were used for a

reference liver fibrosis assessment; accordingly, we included laboratory data obtained within 7 days from the Gd-EOB-DTPA-enhanced MRI study date to minimize the influence of factors other than liver fibrosis on the AST and platelet levels. However, this effort could not remove all bias.

In conclusion, this study was the first study to evaluate liver fibrosis by calculating CV values in liver parenchyma. CV values were well correlated with APRI and FIB-4 index. Among patients with CHB, the CV values differed significantly between those with non-significant and significant liver fibrosis. As such, a CV map on gadoteric acid-enhanced MRI could render the possibility of quantitatively measuring hepatic fibrosis in patients with CHB.

REFERENCES

1. Korean Liver Cancer Study Group (KLCSG); National Cancer Center, Korea (NCC). 2014 Korean Liver Cancer Study Group-National Cancer Center Korea practice guideline for the management of hepatocellular carcinoma. *Korean J Radiol* 2015;16:465-522
2. Ganem D, Prince AM. Hepatitis B virus infection--natural history and clinical consequences. *N Engl J Med* 2004;350:1118-1129
3. Afdhal NH, Nunes D. Evaluation of liver fibrosis: a concise review. *Am J Gastroenterol* 2004;99:1160-1174
4. Yoon JH, Park JW, Lee JM. Noninvasive diagnosis of hepatocellular carcinoma: elaboration on Korean Liver Cancer Study Group-National Cancer Center Korea Practice Guidelines compared with other guidelines and remaining issues. *Korean J Radiol* 2016;17:7-24
5. Bedossa P, Dargère D, Paradis V. Sampling variability of liver fibrosis in chronic hepatitis C. *Hepatology* 2003;38:1449-1457
6. Cadranel JF, Rufat P, Degos F. Practices of liver biopsy in France: results of a prospective nationwide survey. For the Group of Epidemiology of the French Association for the Study of the Liver (AFEF). *Hepatology* 2000;32:477-481
7. Kim BK, Kim SA, Park YN, Cheong JY, Kim HS, Park JY, et al. Noninvasive models to predict liver cirrhosis in patients with chronic hepatitis B. *Liver Int* 2007;27:969-976
8. Motosugi U, Ichikawa T, Sou H, Sano K, Tominaga L, Kitamura T, et al. Liver parenchymal enhancement of hepatocyte-phase images in Gd-EOB-DTPA-enhanced MR imaging: which biological markers of the liver function affect the enhancement? *J Magn Reson Imaging* 2009;30:1042-1046
9. Wai CT, Greenson JK, Fontana RJ, Kalbfleisch JD, Marrero JA, Conjeevaram HS, et al. A simple noninvasive index can predict both significant fibrosis and cirrhosis in patients with chronic hepatitis C. *Hepatology* 2003;38:518-526
10. Shin WG, Park SH, Jang MK, Hahn TH, Kim JB, Lee MS, et al. Aspartate aminotransferase to platelet ratio index (APRI) can predict liver fibrosis in chronic hepatitis B. *Dig Liver Dis*

- 2008;40:267-274
11. Xiao G, Yang J, Yan L. Comparison of diagnostic accuracy of aspartate aminotransferase to platelet ratio index and fibrosis-4 index for detecting liver fibrosis in adult patients with chronic hepatitis B virus infection: a systemic review and meta-analysis. *Hepatology* 2015;61:292-302
 12. Geier A, Dietrich CG, Voigt S, Kim SK, Gerloff T, Kullak-Ublick GA, et al. Effects of proinflammatory cytokines on rat organic anion transporters during toxic liver injury and cholestasis. *Hepatology* 2003;38:345-354
 13. Kim SM, Heo SH, Kim JW, Lim HS, Shin SS, Jeong YY, et al. Hepatic arterial phase on gadoteric acid-enhanced liver MR imaging: a randomized comparison of 0.5 mL/s and 1 mL/s injection rates. *Korean J Radiol* 2014;15:605-612
 14. Tsuboyama T, Onishi H, Kim T, Akita H, Hori M, Tatsumi M, et al. Hepatocellular carcinoma: hepatocyte-selective enhancement at gadoteric acid-enhanced MR imaging--correlation with expression of sinusoidal and canalicular transporters and bile accumulation. *Radiology* 2010;255:824-833
 15. Van Beers BE, Pastor CM, Hussain HK. Primovist, Eovist: what to expect? *J Hepatol* 2012;57:421-429
 16. Kim H, Park SH, Kim EK, Kim MJ, Park YN, Park HJ, et al. Histogram analysis of gadoteric acid-enhanced MRI for quantitative hepatic fibrosis measurement. *PLoS One* 2014;9:e114224
 17. Kanki A, Tamada T, Higaki A, Noda Y, Tanimoto D, Sato T, et al. Hepatic parenchymal enhancement at Gd-EOB-DTPA-enhanced MR imaging: correlation with morphological grading of severity in cirrhosis and chronic hepatitis. *Magn Reson Imaging* 2012;30:356-360
 18. Tamada T, Ito K, Higaki A, Yoshida K, Kanki A, Sato T, et al. Gd-EOB-DTPA-enhanced MR imaging: evaluation of hepatic enhancement effects in normal and cirrhotic livers. *Eur J Radiol* 2011;80:e311-e316
 19. Sato Y, Matsushima S, Inaba Y, Sano T, Yamaura H, Kato M, et al. Preoperative estimation of future remnant liver function following portal vein embolization using relative enhancement on gadoteric acid disodium-enhanced magnetic resonance imaging. *Korean J Radiol* 2015;16:523-530
 20. Huh J, Kim SY, Yeh BM, Lee SS, Kim KW, Wu EH, et al. Troubleshooting arterial-phase MR images of gadoteric acid disodium-enhanced liver. *Korean J Radiol* 2015;16:1207-1215
 21. Li C, Huang R, Ding Z, Gatenby JC, Metaxas DN, Gore JC. A level set method for image segmentation in the presence of intensity inhomogeneities with application to MRI. *IEEE Trans Image Process* 2011;20:2007-2016
 22. Roth M, Obaidat A, Hagenbuch B. OATPs, OATs and OCTs: the organic anion and cation transporters of the SLC0 and SLC22A gene superfamilies. *Br J Pharmacol* 2012;165:1260-1287
 23. Chen ZS, Tiwari AK. Multidrug resistance proteins (MRPs/ABCCs) in cancer chemotherapy and genetic diseases. *FEBS J* 2011;278:3226-3245
 24. Leonhardt M, Keiser M, Oswald S, Kühn J, Jia J, Grube M, et al. Hepatic uptake of the magnetic resonance imaging contrast agent Gd-EOB-DTPA: role of human organic anion transporters. *Drug Metab Dispos* 2010;38:1024-1028
 25. Schmitt M, Kubitz R, Wettstein M, vom Dahl S, Häussinger D. Retrieval of the MRP2 gene encoded conjugate export pump from the canalicular membrane contributes to cholestasis induced by tert-butyl hydroperoxide and chloro-dinitrobenzene. *Biol Chem* 2000;381:487-495
 26. Beuers U, Bilzer M, Chittattu A, Kullak-Ublick GA, Keppler D, Paumgartner G, et al. Tauroursodeoxycholic acid inserts the apical conjugate export pump, MRP2, into canalicular membranes and stimulates organic anion secretion by protein kinase C-dependent mechanisms in cholestatic rat liver. *Hepatology* 2001;33:1206-1216
 27. Atzori L, Poli G, Perra A. Hepatic stellate cell: a star cell in the liver. *Int J Biochem Cell Biol* 2009;41:1639-1642
 28. Chen BB, Hsu CY, Yu CW, Wei SY, Kao JH, Lee HS, et al. Dynamic contrast-enhanced magnetic resonance imaging with Gd-EOB-DTPA for the evaluation of liver fibrosis in chronic hepatitis patients. *Eur Radiol* 2012;22:171-180
 29. Tsuda N, Matsui O. Cirrhotic rat liver: reference to transporter activity and morphologic changes in bile canaliculi--gadoteric acid-enhanced MR imaging. *Radiology* 2010;256:767-773
 30. Chon YE, Choi EH, Song KJ, Park JY, Kim DY, Han KH, et al. Performance of transient elastography for the staging of liver fibrosis in patients with chronic hepatitis B: a meta-analysis. *PLoS One* 2012;7:e44930
 31. Shi Y, Guo Q, Xia F, Dzyubak B, Glaser KJ, Li Q, et al. MR elastography for the assessment of hepatic fibrosis in patients with chronic hepatitis B infection: does histologic necroinflammation influence the measurement of hepatic stiffness? *Radiology* 2014;273:88-98
 32. Liu J, Ji Y, Ai H, Ning B, Zhao J, Zhang Y, et al. Liver shear-wave velocity and serum fibrosis markers to diagnose hepatic fibrosis in patients with chronic viral hepatitis B. *Korean J Radiol* 2016;17:396-404
 33. Yoo H, Lee JM, Yoon JH, Lee DH, Chang W, Han JK. Prospective comparison of liver stiffness measurements between two point shear wave elastography methods: virtual touch quantification and elastography point quantification. *Korean J Radiol* 2016;17:750-757